Hindawi
Journal of Nanomaterials
Volume 2017, Article ID 4875319, 10 pages
https://doi.org/10.1155/2017/4875319

Research Article

Surface Modification of Carbon Nanofibers and Graphene Platelets Mixtures by Plasma Polymerization of Propylene

Carlos Andrés Covarrubias-Gordillo,[1] Florentino Soriano-Corral,[1] Carlos Alberto Ávila-Orta,[1] Victor Javier Cruz-Delgado,[1] María Guadalupe Neira-Velázquez,[1] Ernesto Hernández-Hernández,[2] José Francisco Hernández-Gámez,[2] and Patricia Adriana De León-Martínez[1]

[1]*Centro de Investigación en Química Aplicada, Blvd. Enrique Reyna 140, 25294 Saltillo, COAH, Mexico*
[2]*CONACYT, Centro de Investigación en Química Aplicada, Blvd. Enrique Reyna 140, 25294 Saltillo, COAH, Mexico*

Correspondence should be addressed to Florentino Soriano-Corral; florentino.soriano@ciqa.edu.mx and Carlos Alberto Ávila-Orta; carlos.avila@ciqa.edu.mx

Received 17 February 2017; Accepted 11 June 2017; Published 25 July 2017

Academic Editor: Andrew R. Barron

Carbon nanofibers (CNFs), graphene platelets (GPs), and their mixtures were treated by plasma polymerization of propylene. The carbon nanoparticles (CNPs) were previously sonicated in order to deagglomerate and increase the surface area. Untreated and plasma treated CNPs were analyzed by dynamic light scattering (DLS), transmission electron microscopy (TEM), Fourier transform infrared spectroscopy (FTIR), Raman spectroscopy, and thermogravimetric analysis (TGA). DLS analysis showed a significant reduction of average particle size, due to the sonication pretreatment. Plasma polymerized propylene was deposited on the CNPs surface; the total amount of polymerized propylene was from 4.68 to 6.58 wt-%. Raman spectroscopy indicates an increase in the sp^3 hybridization of the treated samples, which suggest that the polymerized propylene is grafted onto the CNPs.

1. Introduction

Carbon atoms have a specific behavior that allows different electron configurations, known as hybridization, sp^2 hybridization being responsible for the formation of two-dimensional sheets formed by carbon atoms arranged in hexagons, known as graphene [1]. This hexagonal pattern is responsible for its unique properties such as high electrical and thermal conductivity and high mechanical strength [2–4], making it ideal to improve the properties of several polymer matrices. Graphene is considered the basic structure of various allotropes of carbon, such as carbon nanotubes (CNTs), fullerenes, carbon nanofibers (CNFs), and graphene platelets (GPs) [1, 5–8].

One of these allotropes that has generated particular interest, specifically for industrial scale, is the CNFs, due to their low cost and excellent physicochemical properties. Besides, they are easy to process and disperse in different polymer systems [9, 10]. Typically, these nanofilaments formed by stacked graphene sheets from the catalytic decomposition of certain hydrocarbons have diameters ranging from 2 to 100 nm and lengths from 5 to 100 μm [11, 12]. Another allotrope of interest is the GPs, which are constituted by a low number of stacked graphene sheets (reaching up to 10 nm of thickness) [13] forming a planar structure. This structure and its ultrahigh aspect ratio provide to GPs extraordinary properties such as high thermal conductivity and high mechanical strength [6, 14].

The addition of CNPs into polymer matrices has shown a marked improvement in the physicochemical properties of the nanocomposites; moreover, there is a tendency to add a mixture of two or more different carbon nanoparticles aiming to obtain a synergistic effect in the final properties of polymer nanocomposites [6, 15–19]. For example, when one-dimensional carbon nanostructures (CNTs or CNFs) are intercalated with GPs or graphene (2D), a 3D network is promoted, which allows a greater interaction and a better

dispersion and spatial distribution of the CNPs in the polymer matrix [18, 20]. On the other hand, surface modification or functionalization of carbon nanoparticles is a strategy to improve the interfacial adhesion with the matrix and also to get better dispersion in the polymer [21, 22]. In general, CNPs can be modified covalently or by physical interactions. In the first case, functional groups are bonded chemically on the surface of the CNPs [23], while electrostatic interactions or van der Waals forces [21] act as linkages in the second case. Considering the properties of the CNPs associated with its structure, a good selection of the modification method is necessary, to affect as little as possible the structure of the CNPs. In this sense, the surface modification of CNPs by means of plasma polymerization represents an innovative and sustainable alternative, because it is fast and simple and is performed in the absence of solvents (dry process). For example, CNPs have been coated with an ultrathin polypropylene layer when propylene monomer in the vapor phase was fed into and polymerized in a plasma reactor and deposited as an ultrathin film on the surface of the CNPs [24, 25]. On another study, Zhao et al. produced a change in the surface properties of CNTs via plasma treatment using an argon-oxygen gas mixture as feed into the plasma reactor. New chemical groups, such as C-O, grafted on the CNTs surface, and a reduction of the sp^2-hybridization were observed [26]. Neira-Velázquez et al. achieved the deposition of ultrathin polyacrylic acid film on the CNFs surface, and, according to the Raman results, it might be presumed that this nanofilm could be covalently bonded on the surface of nanofiber [27]. However, a slight decrease in the sp^2 hybridization was observed after the plasma treatment, which, on the other hand, indicated that polymerized gases such as acrylic acid tend to produce a coating without significantly affecting the surface structure of the substrate. In a similar way, other researches have been treated CNPs by plasma polymerization using different monomers to coat carbon nanostructures [24, 28, 29]. Plasma technology also has been used recently to modified graphene materials and novel properties have been found as a result of this plasma treatment such as photoluminescence [30] and semiconductivity [31] and selective detection for biosensors [32, 33].

This study is focused on the surface modification of graphene platelets and carbon nanofibers mixtures by plasma polymerization using propylene monomer as feed into the plasma reactor in order to deposit an ultrathin polypropylene film on the surface of these carbon nanostructures.

2. Experimental Section

2.1. Materials. The CNFs were purchased from Pyrograph Products, Inc., USA, with an average diameter of 100 nm and a specific surface area of 41 $m^2\,g^{-1}$, while GPs were obtained from Cheap Tubes, USA, with 1–3 μm in diameter, 10–12 layers of graphene, and a specific surface area of 600–750 $m^2\,g^{-1}$. Propylene monomer from Sigma-Aldrich was used as received.

2.2. Methodology. The CNPs were first sonicated in a glass reactor, to induce the deagglomeration of these carbon nanoparticles [34–36], as follows: 1 g of CNPs (CNFs and GPs, as well as the CNFs : GPs mixtures, in the following ratios by weight: 9 : 1, 8 : 2, or 7 : 3) was introduced in a glass reactor arranged with a sonotrode (see Figure 1) and sonicated at 20 kHz for 30 min in an air atmosphere. To improve the efficiency of functionalization, magnetic agitation was included.

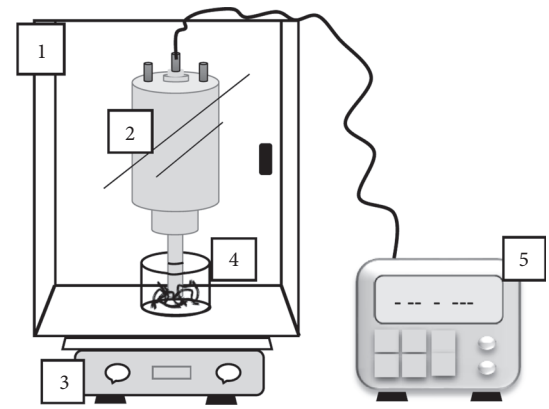

Figure 1: Schematic representation of the sonication system used to reduce the average particle size and particle size distribution of CNPs agglomerates. (1) Sound insulating chamber, (2) ultrasound horn, (3) magnetic agitation, (4) reactor with lid, and (5) ultrasound generator.

A plasma polymerization reactor, reported by Neira-Velázquez et al. [27], was used for the surface modification of the CNPs. The plasma treatment was carried out as follows: 2 g of CNPs was introduced in the glass reactor and the system was put under vacuum. Then, a flow of propylene was fed into the reactor as a result of maintaining a constant pressure (vacuum) of 20 Pa inside the reactor. The plasma treatment condition was 60 W for 60 min.

2.3. Characterization. A Zetasizer Nano S90, Dynamic Light Scattering (DLS) instrument was used for evaluating particle size distribution of CNPs before and after sonication. 1 mg of each CNPs was added to 10 mL of xylene and mechanically stirred for the dispersion test.

A Magna Nicolet 550 infrared spectrophotometer (FTIR) was used for analysis of untreated and plasma modified CNPs within 4000 to 400 cm^{-1}. Previously, the samples were dried in a vacuum oven at 100°C for 15 h, and thereafter they were supported in KBr disks.

A TA Instruments thermogravimetric analyzer (TGA) was used to examine the thermal stability of samples within a temperature range of 30 to 600°C, at 10°C/min, under nitrogen flow of 50 mL/min. From 600 to 800°C, the nitrogen flow was changed to oxygen flow, at the same 50 mL/min, in order to favor the total oxidation of the sample.

For analysis by transmission electron microscopy (TEM), a TITAN 80–300 kV microscope equipped with field emission gun and with a symmetrical condenser-objective lens type S-TWIN (Cs = 1.33 nm) was used. Images obtained by HRTEM have been registered in a CCD camera near the Scherzer focus.

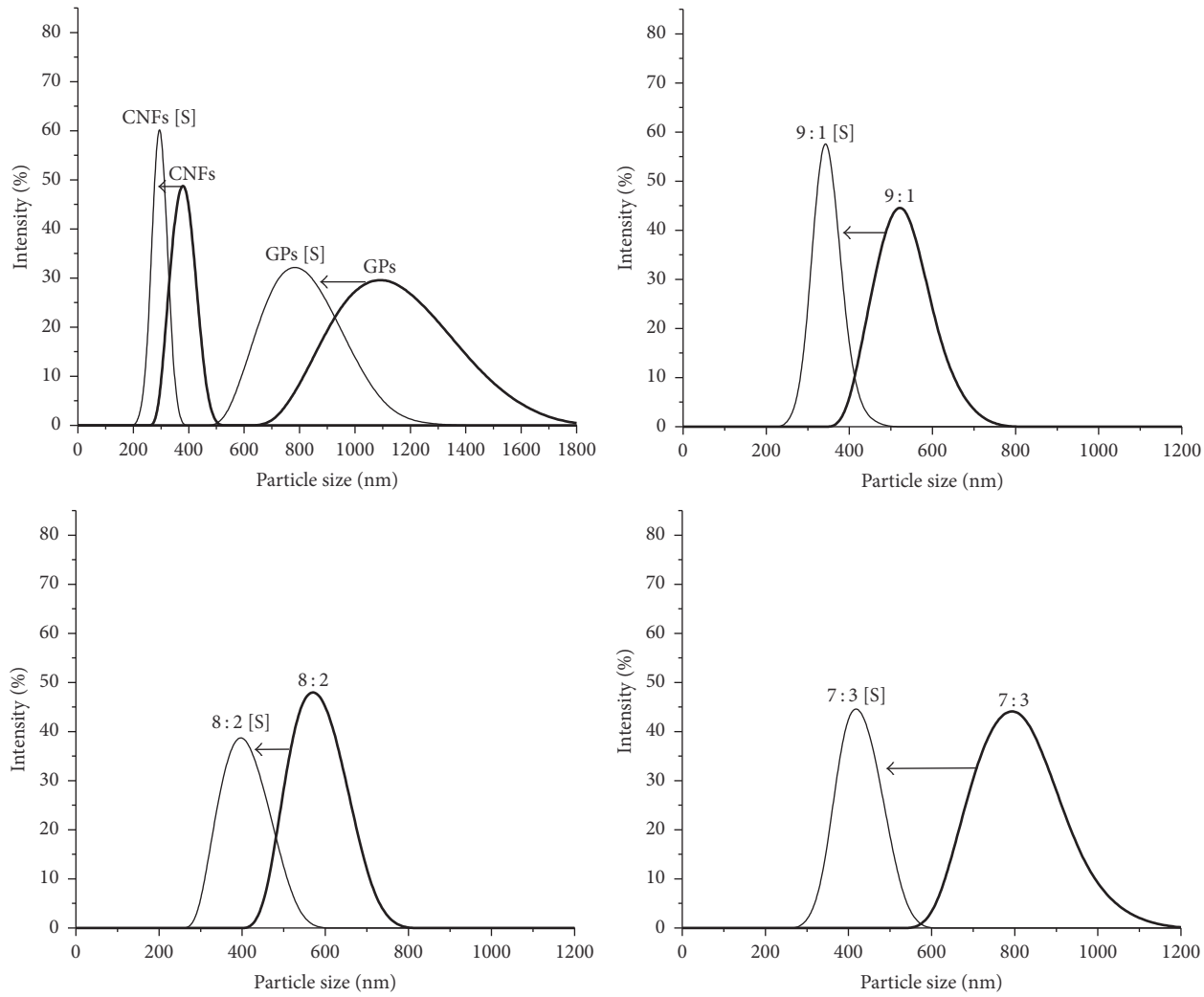

Figure 2: Particle size distribution of samples: before sonication, labeled as CNFs, GPs, and the corresponding CNFs : GPs mixtures as 9 : 1, 8 : 2, and 7 : 3; and after sonication, labeled equal, but followed by a [S].

To assess the hybridization degree of the untreated and treated CNPs, a Horiba Scientific Micro Raman Xplora spectrophotometer was used from 1000 to 4000 cm^{-1}. A laser with 514 nm and 10x was used to realize the Raman analysis.

3. Results and Discussion

3.1. Deagglomeration of CNPs Analyzed by DLS. Figure 2 shows the particle size distribution (PSD) of the CNPs before and after sonication. Samples before sonication are labeled as CNFs, GPs, and the corresponding CNFs : GPs mixtures as 9 : 1, 8 : 2, and 7 : 3. Sonicated samples are labeled the same, but followed by [S].

It can clearly be observed that, in all cases, the particle size at the peak decreases with the sonication treatment; and, in all cases as well, the width of the particle size distribution curves decreases with the sonication treatment. This might indicate that sonication produces a certain degree of size homogenization as well as a smaller average particle size.

This decrease in average particle size is associated with an increase in the particle Theoretical Surface Area (TSA). TSA was calculated using

$$\text{TSA} = a\frac{b}{c}, \tag{1}$$

where $a = \pi D^2$ and "a" is the TSA of 1 nanoparticle with diameter "D". $b = 1/\rho$ and "b" is the total volume of 1 g of CNPs with density "ρ". $c = (4/3)\pi r^3$ and "c" is the volume of 1 nanoparticle with radius "r".

Thus, b/c is equal to the number of CNPs per 1 g of sample.

For calculations with (1), all particles were assumed as spherical, and densities were taken from the supplier as $\rho_{\text{CNFs}} = 1.95 \times 10^6\ \text{g m}^{-3}$ and $\rho_{\text{CPs}} = 0.04 \times 10^6\ \text{g m}^{-3}$. The densities of CNFs and GPs mixtures were calculated from these. The results are summarized in Table 1.

Graphene deagglomeration by means of sonication in an solvent medium has been studied by several authors [37–39]. However, in our air atmosphere sonicate system, the PSD of

Table 1: Particle size at the peak of the size distribution curves of Figure 2 and theoretical surface area of each particle group.

CNPs	As received, particle size [nm]	Sonicated, particle size [nm]	[(a)]TSA [m^2/g], as received samples	TSA [m^2/g], sonicated samples
CNFs	540	290	8.2	[(b)]10.6 *(29%)*
GPs	1075	790	139.8	189.9 *(35%)*
CNFs/GPs 9 : 1	520	340	34.2	52.1 *(53%)*
CNFs/GPs 8 : 2	570	400	56.8	81.5 *(43%)*
CNFs/GPs 7 : 3	795	415	59.3	113.1 *(90%)*

[(a)]TSA: theoretical surface area; [(b)]percent increase in TSA after sonication, in parenthesis.

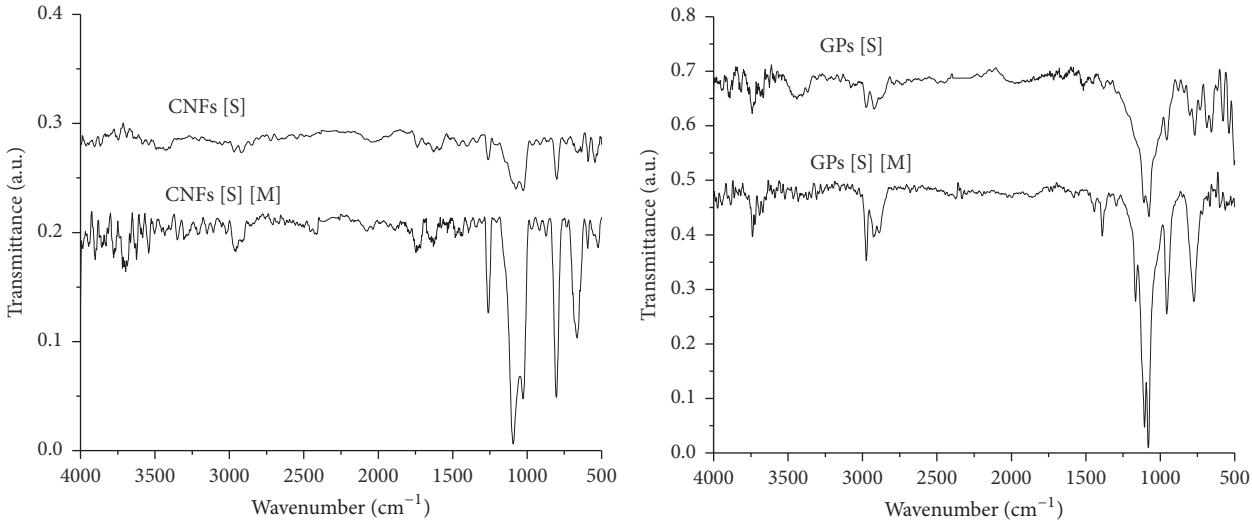

Figure 3: FTIR spectra of untreated and plasma treated of CNPs.

CNPs decreases, since the ultrasound waves are propagated through the gas (atmospheric air) and hit on the surface of the CNPs. The initial impact causes a suspension of the CNPs in the air and then a fluidized bed is formed. Within the fluidized bed, agglomerates absorbed the impact shock of ultrasound waves, creating a vibration in their body, resulting in exfoliation/fragmentation [36].

Such exfoliation is identified as CNPs with smaller average size in the DLS analysis (see Table 1). Also in Table 1, it is observed that the particle size decreases and the TSA increases, due to the increase in the number of particles per gram. With respect to the increment of TSA in percentage, the highest percentages were obtained for NPs combinations (specifically the combination of CNFs : GPs in a ratio of 7 : 3 reached an increase of 90%); this indicates a more effective deagglomeration treatment when CNFs and GPs are used together. It is suggested that impact shock of ultrasound waves occurs due to the increment in the interactions between the CNPs in the fluidized bed, probably due to the different morphology (size and shape) of the agglomerates in the system, encouraging the passage of the necessary ultrasound waves vibrations to deagglomerate all CNPs.

3.2. Infrared Analysis. FTIR spectra of sonicated CNFs and GPs (marked with an [S] at the end), and sonicated plus plasma treated CNFs and GPs (marked with an [S] [M] at the end), are presented in Figure 3. The signals at 2800–3000 cm^{-1}, characteristic of a symmetric C-H stretching, appear in both spectra (with and without plasma treatment). However, a slightly higher intensity is observed in the plasma modified CNPs, due to a higher concentration of C-H bonding present on the surface of the CNPs. It is common to find signals of low intensity in the untreated CNPs, which are organic molecules (hydrocarbons) that remain on the surface of CNPs

The band at 1633 cm^{-1} appears in the CNFs spectra, but not for the case of the GPs. This could be related to the adsorption of water from the environment [40]. A noticeable increase is observed in the bands at 1450 and 1440 cm^{-1} after the plasma treatment, particularly in the GPs, attributed to the presence of -CH_2- groups. Likewise, a noticeable increase is observed in the bands at 1255 cm^{-1} after the plasma treatment, particularly in the CNFs, which is associated with the appearance of tertbutyl groups. In addition, the band at 1098 cm^{-1} shows an increase, which is attributed to the vibrations produced by the stretching and swing modes of C-C, and bends and twists of C-H. Another increment is observed in the band at 660 cm^{-1} for trans-alkene disubstituted groups and at 800 cm^{-1} which indicates the vibrations of stretching of C-H and C-C, and oscillations of CH_2 [41].

All changes in these signals are associated with the chemical groups deposited on the surface on CNPs by the plasma treatment. Finally, a significant change is observed in the bands at 1740 cm^{-1} after the plasma treatment, particularly in the CNFs, indicating that they suffered oxidation either during or after the plasma treatment. This is a common phenomenon in plasma modification, because after treatment there are several active sites remaining on the surface of carbon nanoparticles, and, after treatment, they react with ambient oxygen.

The modification on the carbon nanoparticles made via the plasma treatment with propylene can be ascertained as a result of the changes in the FTIR signals above. However, none of these signals appears in the form of polypropylene (PP). According to the infrared analysis, it is suggested that the PP is in the form of a crosslinked homopolymer, due to the significant increase in the signal characteristic of the tertbutyl group. It is well known that the plasma polymerization promotes crosslinked structures, due to the multiple reactive species that are generated during the process. This is reflected in the decomposition temperature obtained by TGA, higher than the decomposition temperature of polypropylene (300°C) [42–44].

3.3. Thermal Stability. In Figure 4, TGA thermograms are showed for the untreated and plasma treated CNFs, GPs, and the CNFs : GPs mixtures with an 9 : 1, 8 : 2, and 7 : 3 weight ratios. First, it is observed that there is a noticeable difference between the CNFs and GPs, either untreated or treated. With respect to the untreated carbon nanoparticles, when they are heated up to 600°C, the weight loss of the CNFs is almost 1%, whereas the weight loss of the GPs reaches up to 11%. The weight loss of the untreated GPs is assumed to be associated with organic material adsorbed on the particles surface during their synthesis. On the other hand, when the plasma treated carbon nanoparticles are heated up to 600°C, an additional weight loss of 4.68 and 6.58% is observed for CNFs and GPs, respectively. That is, when heated in a N_2 atmosphere, the weight loss of the GPs is greater than that of the CNFs. On the other hand, the weight loss of untreated mixtures of CNFs : GPs (9 : 1, 8 : 2, and 7 : 3) shows values of 9, 7, and 4%, respectively, while the additional weight losses observed in the treated samples are 4.92, 5.07, and 5.54%, respectively, probably due to the increase in the theoretical surface area of the mixtures (see Table 1). The additional weight loss in the plasma treated CNFs, GPs, and mixtures of them is entirely attributed to the polymeric material deposited on the particles surface during the propylene plasma treatment.

3.4. Morphology by TEM. Figure 5 presents TEM images of untreated and plasma treated CNPs. Figure 5(a) shows a CNFs segment in which a structure known as CNFs stacked cups (Endo et al. in 2003) can be observed [45]. Shanmugam and Gedanken observed CNTs with similar structure, which they called "bamboo" structure [46]. The flat surface is inclined with respect to the axial direction of the fiber, thereby exposing the edges of the plane of the CNFs, generating a greater surface area and facilitating the surface modification thereof. Furthermore, it is observed that the presence of a thin homogeneous layer of about 2 to 3 nm is associated with amorphous carbon on the surface of the CNFs, being this common due to the synthesis method used [47]. At a lower magnification (Figure 5(b)), it can be observed that the surface of the CNFs is smooth and without any noticeable variations on the diameter along the fiber. On the contrary, Figure 5(c) shows a segment of plasma treated CNFs, where plasma polymerized PP is anchored on the CNFs surface and is denoted as clusters (marked with red arrows). However, these clusters have a higher density and break the apparent smoothness observed in the untreated CNFs (seen in Figure 5(b)) [48, 49]. Figure 5(d) shows an agglomerate of untreated GPs. Red circles indicate GPs with thickness less than 10 nm, whereas the squares indicate GPs with thickness more than 15 nm. Most GPs are below 10 nm in the agglomerate; the dark areas have a stack of GPs, while lighter areas indicate the presence of thinner stacked lamellae. In addition, it is noteworthy that the electron diffraction analysis of the CNPs, results in a characteristic interplanar distance of 3.5 Å between graphene layers [50, 51]. Figure 5(e) shows plasma treated GPs, where clusters (in red circles) might suggest the evidence of PP grafted on its surface.

3.5. Dispersion Test. Dispersion tests in xylene can provide an idea if the plasma modification has been achieved on the CNPs surface. Figure 6 shows images of the untreated and plasma treated carbon nanoparticles analyzed in this study (CNFs, GPs, and the CNFs : GPs mixtures at 9 : 1, 8 : 2, and 7 : 3 ratios), taken after 24 h in xylene of 5 vials with untreated CNPs treated and another 5 with CNPs untreated. The untreated CNPs show no interaction with the solvent, and they sediment immediately. The plasma treated CNPs, on the other hand, remain dispersed for much longer times, suggesting an increase in interaction between the CNPs and the solvent, where probably methyl groups of polypropylene (PP) increase this interaction.

In addition, an increase was observed in the interaction of CNPs with the solvent when concentration of GPs gets higher, despite having similar degree of modification.

3.6. Hybridization Degree by Raman Spectroscopy. The hybridization degree of the untreated and plasma treated samples was calculated via the D (in 1345 cm^{-1}) and G (1575 cm^{-1}) bands, using Raman spectroscopy. Several authors have proposed that the ratio of these intensity bands (I_D/I_G) can be used for characterizing the degree of structural disorder present on the surface of the CNPs, which is important because it may indicate the degree of modification [52–57]. Figure 7 shows the Raman spectra, in the high frequency region (1100–1800 cm^{-1}) of the untreated and plasma treated CNFs and GPs. CNFs signal shows a slight increase in the intensity of the D band, which is related to the amount of defects on the surface of the CNPs, while, for GPs, the D band remains without any significant change; however, a considerable decrease of the G band is produced, denoting a change of hybridization from sp^2 to sp^3. Table 2 shows the values obtained by Raman spectroscopy for untreated CNPs (denoted by the [S] extension) and plasma

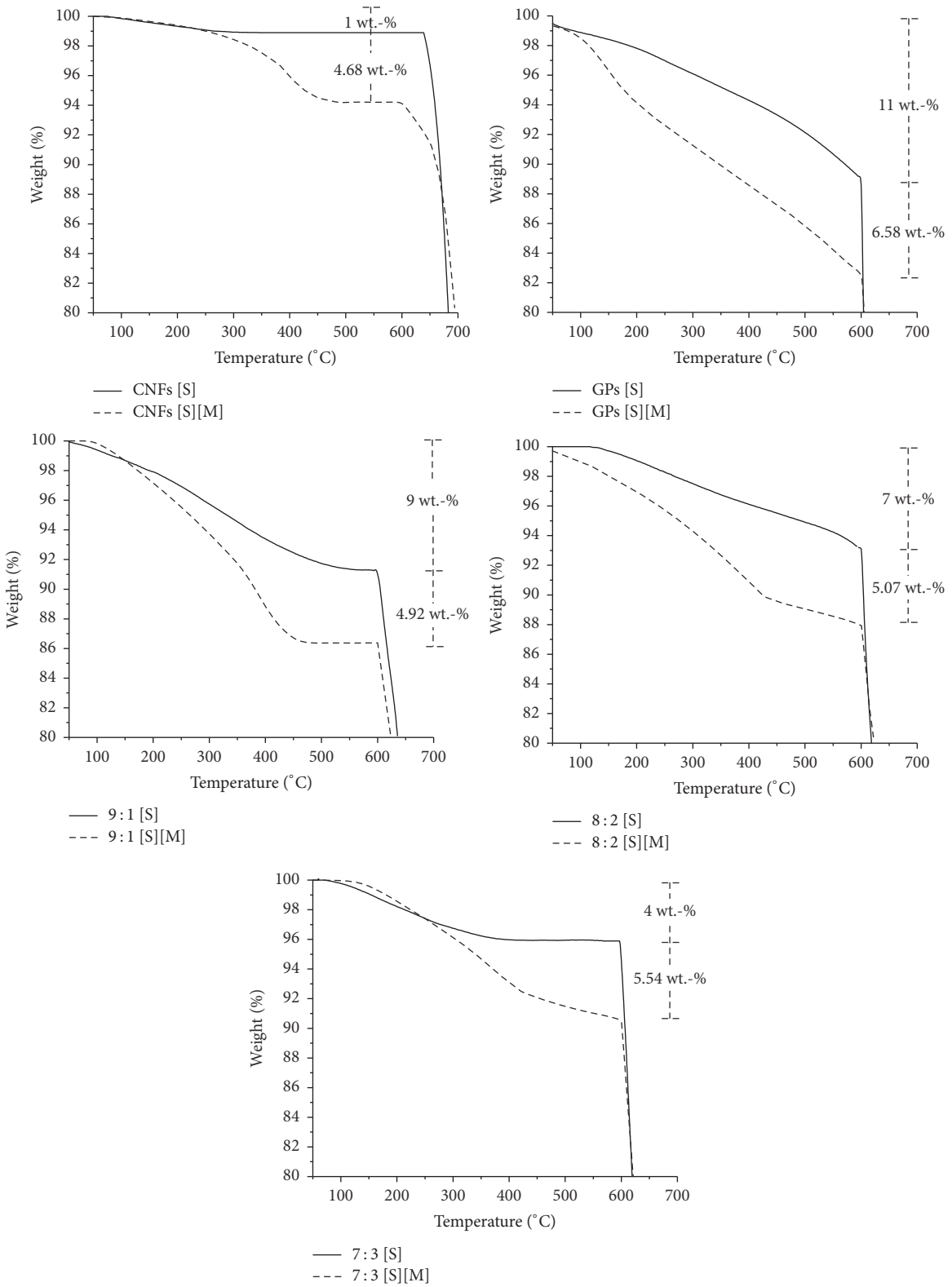

Figure 4: Thermogravimetric curves of untreated and treated CNFs, GPs and samples of CNFs : GPs at ratios of 9 : 1, 8 : 2, and 7 : 3.

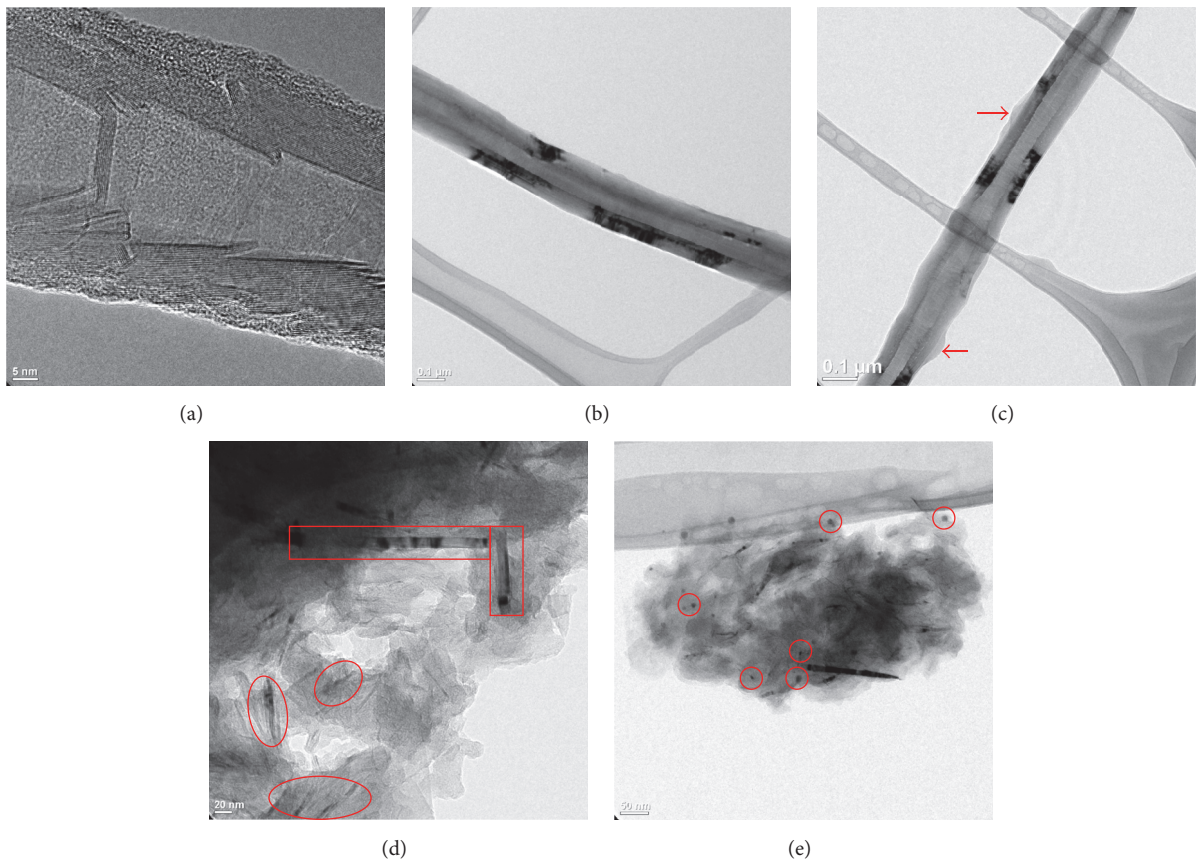

FIGURE 5: TEM images of CNPs. (a) Stacked cups morphology of CNFs, (b) plasma untreated CNFs, (c) treated CNFs, (d) untreated GPs, and (e) plasma treated GPs.

FIGURE 6: Dispersion test in xylene of CNPs. Left: untreated CNPs. Right: plasma treated CNPs after 24 h. (a) CNFs, (b) GPs, (c) 9 : 1, (d) 8 : 2, and (e) 7 : 3.

treated CNPs (denoted by the [S] [M] extension), where I_D/I_G increases as a function of GPs content, showing that the GPs presents a higher hybridization change from sp^2 to sp^3.

Values of I_D/I_G from Table 2 and values of weight loss from TGA analysis are plotted in Figure 8 versus the CNFs : GPs ratio, from 100 : 0 to 0 : 100. The I_D/I_G value and the amount of weight loss by TGA increase with the GPs content of the plasma treated CNPs, suggesting that GPs have a greater proportion of covalent modification than CNFs; that is, the percentage of deposited PP depends of the specific surface area exposed by the CNPs (or exposed sp^2 hybridization

Table 2: Summary of I_D/I_G values of all samples obtained by Raman spectroscopy.

NPCs	I_D	I_G	I_D/I_G	$\Delta I_D/I_G$
CNFs [S]	0.14	1	0.14	0.07
CNFs [S] [M]	0.19	0.94	0.21	
9 : 1 [S]	0.33	1	0.33	0.14
9 : 1 [S] [M]	0.46	0.96	0.47	
8 : 2 [S]	0.26	1	0.26	0.19
8 : 2 [S] [M]	0.43	0.95	0.45	
7 : 3 [S]	0.34	1	0.34	0.20
7 : 3 [S] [M]	0.50	0.94	0.54	
GPs [S]	0.80	1	0.80	0.32
GPs [S] [M]	0.80	0.71	1.12	

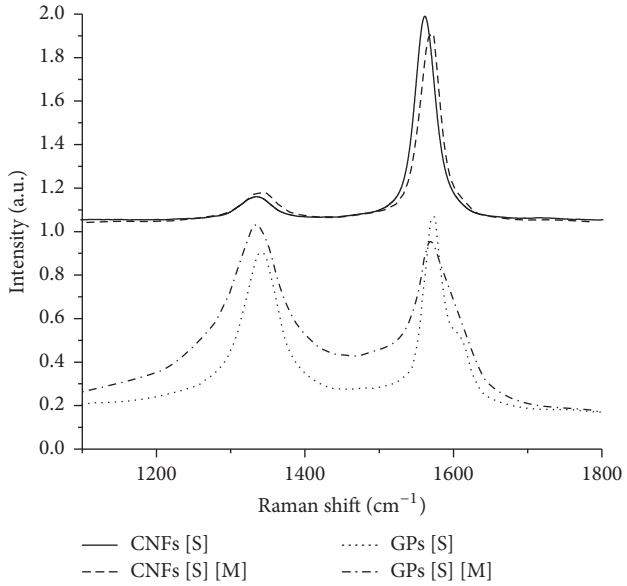

Figure 7: Raman spectroscopy of treated and untreated CNFs and GPs.

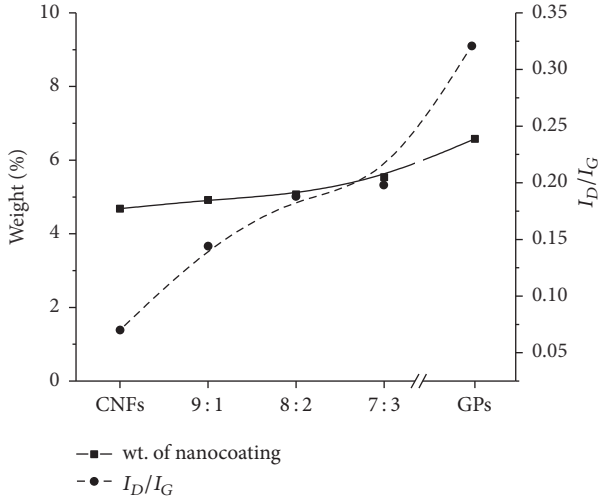

Figure 8: Changes in the I_D/I_G ratio and TGA loss weight percentage for each CNPs and its mixtures.

sites). Therefore, the type of surface modification (covalent or physical) depends of the number of sites that can be chemically modified.

The hybridization change and the amount of polymer deposited are related by the TSA of the CNPs. A higher TSA not only represents a larger area where the polymer can be deposited but also represents a greater exposure of sp^2 hybridization points by the CNPs allowing covalent bonds between the polymer and the surface of the CNPs (denoted by the hybridization change). For this reason, GPs with larger TSA than CNFs generate more covalent interaction with the polymer, as well as a higher percentage of polymer to be deposited on its surface.

4. Conclusions

The results obtained by sonication in gas phase of the CNPs indicated a lower agglomeration, generating CNPs with more TSA; specifically the combination of CNFs : GPs in a ratio of 7 : 3 reached an increase of 90%, indicating a more effective deagglomeration treatment when CNFs and GPs are used together.

A thin film of PP was covalently deposited by plasma polymerization on the surface of carbon nanoparticles. This is reflected in the hybridization change from sp^2 to sp^3 by Raman spectroscopy, among other techniques. The degree of deposition is analyzed with the ratio of I_D/I_G bands. The band analysis shows greater covalent interaction for the GPs and the CNFs : GPs mixtures, due to the higher TSA exposed (or exposed sp^2 hybridization sites) in relation to the CNFs. The amount of deposited polymer coating is not reflected directly in the hybridization change (from sp^2 to sp^3). This change reflects only the covalent interaction of the coating and CNPs, regardless of the amount.

Conflicts of Interest

The authors declare that they have no conflicts of interest.

Acknowledgments

Thanks are due to the Mexican Council of Science and Technology (CONACyT) for the support through the Project

207450-12. Finally, the authors are grateful for technical assistance from E. Diaz Barriga-Castro, M. R. Rangel-Ramirez, G. Mendez-Padilla, F. Zendejo-Rodriguez, M. C. González-Cantú, M. H. Palacios-Mezta, J. G. Rodríguez-Velazquez, and S. Torres-Rincón.

References

[1] K. S. Novoselov, A. K. Geim, S. V. Morozov et al., "Electric field in atomically thin carbon films," *Science*, vol. 306, no. 5696, pp. 666–669, 2004.

[2] V. Singh, D. Joung, L. Zhai, S. Das, S. I. Khondaker, and S. Seal, "Graphene based materials: past, present and future," *Progress in Materials Science*, vol. 56, no. 8, pp. 1178–1271, 2011.

[3] S. Wang, R. Liang, B. Wang, and C. Zhang, "Dispersion and thermal conductivity of carbon nanotube composites," *Carbon*, vol. 47, no. 1, pp. 53–57, 2009.

[4] J. R. Potts, D. R. Dreyer, C. W. Bielawski, and R. S. Ruoff, "Graphene-based polymer nanocomposites," *Polymer*, vol. 52, no. 1, pp. 5–25, 2011.

[5] C. Poole and F. Owens, *Introduction to Nanotechnology*, John Wiley & Sons, Hoboken, NJ, USA, 2003.

[6] S. Araby, N. Saber, X. Ma et al., "Implication of multi-walled carbon nanotubes on polymer/graphene composites," *Materials and Design*, vol. 65, no. 1, pp. 690–699, 2015.

[7] R. Saito, G. Dresselhaus, and M. Dresselhaus, *Physical Properties of Carbon Nanotubes*, Imperial College Press, London, UK, 1998.

[8] J. Bunch, *Mechanical and Electrical Properties of Graphene Sheets [Ph.D. Thesis]*, Cornell University, Ithaca, NY, USA, 2008.

[9] S. Ceccia, D. Ferri, D. Tabuani, and P. L. Maffettone, "Rheology of carbon nanofiber-reinforced polypropylene," *Rheologica Acta*, vol. 47, no. 4, pp. 425–433, 2008.

[10] L. Rassaei, M. Sillanpää, M. J. Bonné, and F. Marken, "Carbon nanofiber-polystyrene composite electrodes for electroanalytical processes," *Electroanalysis*, vol. 19, no. 14, pp. 1461–1466, 2007.

[11] A. Oberlin, M. Endo, and T. Koyama, "Filamentous growth of carbon through benzene decomposition," *Journal of Crystal Growth*, vol. 32, no. 3, pp. 335–349, 1976.

[12] N. Rodriguez, "A review of catalytically grown carbon nanofiber," *Journal of Materials Research*, vol. 8, 1993.

[13] Z. Chen, J. Zou, and H. Cheng, *Nanotubes and Nanosheets: Functionalization and Applications of Boron Nitride and Other Nanomaterials*, CRC Press, Boca Raton, Fla, USA, 2015.

[14] W. Li, A. Dichiara, and J. Bai, "Carbon nanotube-graphene nanoplatelet hybrids as high-performance multifunctional reinforcements in epoxy composites," *Composites Science and Technology*, vol. 74, pp. 221–227, 2013.

[15] M. Safdari and M. S. Al-Haik, "Synergistic electrical and thermal transport properties of hybrid polymeric nanocomposites based on carbon nanotubes and graphite nanoplatelets," *Carbon*, vol. 64, pp. 111–121, 2013.

[16] L. Yue, G. Pircheraghi, S. A. Monemian, and I. Manas-Zloczower, "Epoxy composites with carbon nanotubes and graphene nanoplatelets—dispersion and synergy effects," *Carbon*, vol. 78, pp. 268–278, 2014.

[17] G. Huang, S. Wang, P. Song, C. Wu, S. Chen, and X. Wang, "Combination effect of carbon nanotubes with graphene on intumescent flame-retardant polypropylene nanocomposites," *Composites Part A: Applied Science and Manufacturing*, vol. 59, pp. 18–25, 2014.

[18] P. Song, L. Liu, S. Fu et al., "Striking multiple synergies created by combining reduced graphene oxides and carbon nanotubes for polymer nanocomposites," *Nanotechnology*, vol. 24, no. 12, Article ID 125704, 2013.

[19] Z. Tang, H. Kang, Q. Wei, B. Guo, L. Zhang, and D. Jia, "Incorporation of graphene into polyester/carbon nanofibers composites for better multi-stimuli responsive shape memory performances," *Carbon*, vol. 64, pp. 487–498, 2013.

[20] B. Li and W.-H. Zhong, "Review on polymer/graphite nanoplatelet nanocomposites," *Journal of Materials Science*, vol. 46, no. 17, 2011.

[21] P. Ma, N. Siddiqui, G. Marom, and J. Kim, "Dispersion and functionalization of carbon nanotubes for polymer-based nanocomposites: A review," *Composites Part A: Applied Science and Manufacturing*, vol. 41, no. 10, pp. 1345–1367, 2010.

[22] E. Beyou, S. Akbar, P. Chaumont, and P. Cassagnau, *Synthesis and Applications of Carbon Nanotubes and Their Composites*, vol. 1, InTech, Rijeka, Croatia, 2013.

[23] D. Tasis, N. Tagmatarchis, A. Bianco, and M. Prato, "Chemistry of carbon nanotubes," *Chemical Reviews*, vol. 106, no. 3, pp. 1105–1136, 2006.

[24] C. A. Ávila-Orta, V. J. Cruz-Delgado, M. G. Neira-Velázquez, E. Hernández-Hernández, M. G. Méndez-Padilla, and F. J. Medellín-Rodríguez, "Surface modification of carbon nanotubes with ethylene glycol plasma," *Carbon*, vol. 47, no. 8, pp. 1916–1921, 2009.

[25] B. Ruelle, *Functionalization of Carbon Nanotubes via Plasma Post-discharge Surface Treatment: Implication as Nanofiller in Polymeric Matrices [Ph.D. Thesis]*, University de Mons, Mons, Belgium, 2009.

[26] B. Zhao, L. Zhang, X. Wang, and J. Yang, "Surface functionalization of vertically-aligned carbon nanotube forests by radio-frequency Ar/O 2 plasma," *Carbon*, vol. 50, no. 8, pp. 2710–2716, 2012.

[27] M. G. Neira-Velázquez, E. Hernández-Hernández, L. F. Ramos-deValle et al., "Chemical modification of carbon nanofibers with plasma of acrylic acid," *Plasma Processes and Polymers*, vol. 10, no. 7, pp. 627–633, 2013.

[28] L. Ramos-deValle, M. Neira-Velázquez, and E. Hernández-Hernández, "Surface modification of CNFs via plasma polymerization of styrene monomer and its effect on the properties of ps/cnf nanocomposites," *Journal of Applied Polymer Science*, vol. 107, 2008.

[29] D. Shi, J. Lian, P. He et al., "Plasma deposition of ultrathin polymer films on carbon nanotubes," *Applied Physics Letters*, vol. 81, no. 27, pp. 5216–5218, 2002.

[30] T. Gokus, R. R. Nair, A. Bonetti et al., "Making graphene luminescent by oxygen plasma treatment," *ACS Nano*, vol. 3, no. 12, pp. 3963–3968, 2009.

[31] M. Rybin, A. Pereyaslavtsev, T. Vasilieva et al., "Efficient nitrogen doping of graphene by plasma treatment," *Carbon*, vol. 96, pp. 196–202, 2016.

[32] M. H. Wang, S. L. Liu, Y. C. Zhang et al., "Graphene nanostructures with plasma polymerized allylamine biosensor for selective detection of mercury ions," *Sensors and Actuators B: Chemical*, vol. 203, pp. 497–503, 2014.

[33] Z. Zhang, S. Liu, M. Kang et al., "Graphene nanostructures with plasma-polymerized pyrrole as an adsorbent layer for biosensors," *Microchimica Acta*, vol. 181, no. 9, 2014.

[34] C. A. Ávila-Orta, Z. V. Quiñones-Jurado, M. A. Waldo-Mendoza et al., "Ultrasound-assist extrusion methods for the

fabrication of polymer nanocomposites based on polypropylene/multi-wall carbon nanotubes," *Materials*, vol. 8, no. 11, pp. 7900–7912, 2015.

[35] B. L. España-Sánchez, C. A. Ávila-Orta, F. Padilla-Vaca et al., "Enhanced antibacterial activity of melt processed poly(propylene) Ag and Cu nanocomposites by argon plasma treatment," *Plasma Processes and Polymers*, vol. 11, no. 4, pp. 353–365, 2014.

[36] P. González-morones, R. Yáñez-garcía, D. Navarro-rodríguez, C. Ávila-orta, and M. López-quintanilla, "Estudio de la reducción del tamaño de los aglomerados de MWCNTs por ultrasonido en fase gas y su efecto sobre la modificación superficial por plasma," *Ide@s CONCYTEG*, vol. 6, no. 72, 2011.

[37] R. Durge, R. V. Kshirsagar, and P. Tambe, "Effect of sonication energy on the yield of graphene nanosheets by liquid-phase exfoliation of graphite," in *Proceedings of the 12th Global Congress on Manufacturing and Management, GCMM '14*, pp. 1457–1465, Elsevier, Amsterdam, Netherlands, December 2014.

[38] B. Puangbuppha, P. Limsuwan, and P. Asanithi, "Non-chemically functionalized graphene exfoliated from graphite in water using ultrasonic treatment," in *Proceedings of the 3rd International Science, Social Science, Engineering and Energy Conference, I-SEEC '11*, pp. 1094–1099, February 2012.

[39] A. Ciesielski and P. Samorì, "Graphene via sonication assisted liquid-phase exfoliation," *Chemical Society Reviews*, vol. 43, no. 1, 2014.

[40] T. G. Ros, A. J. Van Dillen, J. W. Geus, and D. C. Koningsberger, "Surface oxidation of carbon nanofibres," *Chemistry-A European Journal*, vol. 8, no. 5, pp. 1151–1162, 2002.

[41] I. Karacan and H. Benli, "The use of infrared-spectroscopy for the structural characterization of isotactic polypropylene fibres," *Tekstil ve Konfeksiyon*, vol. 2, 2011.

[42] F. Avalos-Belmontes, L. F. Ramos-Devalle, E. Ramírez-Vargas, S. Sánchez-Valdes, J. Méndez-Nonel, and R. Zitzumbo-Guzmán, "Nucleating effect of carbon nanoparticles and their influence on the thermal and chemical stability of polypropylene," *Journal of Nanomaterials*, vol. 2012, Article ID 406214, 8 pages, 2012.

[43] S. Luyt, M. Dramicanin, Ž. Antic, and V. Djokovic, "Morphology, mechanical and thermal properties of composites of polypropylene and nanostructured wollastonite filler," *Polymer Testing*, vol. 28, no. 3, 2009.

[44] C. Liao, H. Wong, K. Wai, and K. Yeung, "The development, fabrication, and material characterization of polypropylene composites reinforced with carbon nanofiber and hydroxyapatite nanorod hybrid fillers," *International Journal of Nanomedicine*, vol. 9, 2014.

[45] M. Endo, Y. A. Kim, M. Ezaka et al., "Selective and efficient impregnation of metal nanoparticles on cup-stacked-type carbon nanofibers," *Nano Letters*, vol. 3, no. 6, pp. 723–726, 2003.

[46] S. Shanmugam and A. Gedanken, "Generation of hydrophilic, bamboo-shaped multiwalled carbon nanotubes by solid-state pyrolysis and its electrochemical studies," *Journal of Physical Chemistry B*, vol. 110, 2006.

[47] M. Tsuji, M. Kubokawa, R. Yano et al., "Fast preparation of PtRu catalysts supported on carbon nanofibers by the microwave-polyol method and their application to fuel cells," *Langmuir*, vol. 23, no. 2, pp. 387–390, 2007.

[48] V. Ambrogi, G. Gentile, C. Ducati, M. C. Oliva, and C. Carfagna, "Multiwalled carbon nanotubes functionalized with maleated poly(propylene) by a dry mechano-chemical process," *Polymer*, vol. 53, no. 2, pp. 291–299, 2012.

[49] S. Liu, Z. Wang, G. Lu et al., "Interfacial modification of single-walled carbon nanotubes for high-loading-reinforced polypropylene composites," *Journal of Applied Polymer Science*, vol. 131, no. 3, Article ID 39817, 2014.

[50] Y. Xu, H. Bai, G. Lu, C. Li, and G. Shi, "Flexible graphene films via the filtration of water-soluble," *Journal of the American Chemical Society*, vol. 130, no. 18, 2008.

[51] O. Kharissova and B. Kharisov, "Variations of interlayer spacing in carbon nanotubes," *RSC Advances*, vol. 4, no. 58, 2014.

[52] F. Jiménez, F. Mondragón, and D. López, "Raman characterization of coal chars obtained in a pressurized bed reactor," *Ingenieria y competitividad*, vol. 14, no. 2, 2012.

[53] A. Jorio, E. H. M. Ferreira, F. Stavale et al., "Quantifying defects in graphene via Raman spectroscopy at different excitation energies," *Nano Letters*, vol. 11, no. 8, pp. 3190–3196, 2011.

[54] V. M. Irurzun, M. P. Ruiz, and D. E. Resasco, "Raman intensity measurements of single-walled carbon nanotube suspensions as a quantitative technique to assess purity," *Carbon*, vol. 48, no. 10, pp. 2873–2881, 2010.

[55] E. F. Antunes, A. O. Lobo, E. J. Corat, V. J. Trava-Airoldi, A. A. Martin, and C. Veríssimo, "Comparative study of first- and second-order Raman spectra of MWCNT at visible and infrared laser excitation," *Carbon*, vol. 44, no. 11, pp. 2202–2211, 2006.

[56] O. Beyssac, J.-N. Rouzaud, B. Goffé, F. Brunet, and C. Chopin, "Graphitization in a high-pressure, low-temperature metamorphic gradient: a raman microspectroscopy and HRTEM study," *Contributions to Mineralogy and Petrology*, vol. 143, no. 1, pp. 19–31, 2002.

[57] O. Beyssac, B. Goffé, C. Chopin, and J. N. Rouzaud, "Raman spectra of carbonaceous material in metasediments: a new geothermometer," *Journal of Metamorphic Geology*, vol. 20, no. 9, pp. 859–871, 2002.